Changes in activation sequence of embryonic chick atria correlate with developing myocardial architecture

David Sedmera, Andy Wessels, Thomas C. Trusk, Robert P. Thompson, Kenneth W. Hewett and Robert G. Gourdie

Am J Physiol Heart Circ Physiol 291:1646-1652, 2006. First published May 5, 2006;
doi:10.1152/ajpheart.01007.2005

AJP - Heart and Circulatory Physiology publishes original investigations on the physiology of the heart, blood vessels, and lymphatics, including experimental and theoretical studies of cardiovascular function at all levels of organization ranging from the intact animal to the cellular, subcellular, and molecular levels. It is published 12 times a year (monthly) by the American Physiological Society, 9650 Rockville Pike, Bethesda MD 20814-3991. ISSN: 0363-6135, ESSN: 1522-1539. Visit our website at http://www.the-aps.org/.

Am J Physiol Heart Circ Physiol 291: H1646–H1652, 2006.
First published May 5, 2006; doi:10.1152/ajpheart.01007.2005.

Changes in activation sequence of embryonic chick atria correlate with developing myocardial architecture

David Sedmera,[1,2,3] Andy Wessels,[1] Thomas C. Trusk,[1] Robert P. Thompson,[1] Kenneth W. Hewett,[1] and Robert G. Gourdie[1]

[1]*Department of Cell Biology and Anatomy, Medical University of South Carolina, Charleston, South Carolina;*
[2]*Institute of Animal Physiology and Genetics, Academy of Sciences of the Czech Republic and*
[3]*Department of Anatomy, First Faculty of Medicine, Charles University, Prague, Czech Republic*

Submitted 13 November 2005; accepted in final form 17 April 2006

Sedmera, David, Andy Wessels, Thomas C. Trusk, Robert P. Thompson, Kenneth W. Hewett, and Robert G. Gourdie. Changes in activation sequence of embryonic chick atria correlate with developing myocardial architecture. *Am J Physiol Heart Circ Physiol* 291: H1646–H1652, 2006. First published May 5, 2006; doi:10.1152/ajpheart.01007.2005.—To characterize developmental changes in impulse propagation within atrial musculature, we performed high-speed optical mapping of activation sequence of the developing chick atria using voltage-sensitive dye. The activation maps were correlated with detailed morphological studies using scanning electron microscopy, histology, and whole mount confocal imaging with three-dimensional reconstruction. A preferential pathway appeared during development within the roof of the atria, transmitting the impulse rapidly from the right-sided sinoatrial node to the left atrium. The morphological substrate of this pathway, the bundle of Bachman, apparent from stage 29 onward, was a prominent ridge of pectinate muscles continuous with the terminal crest. Further acceleration of impulse propagation was noted along the ridges formed by the developing pectinate muscles, ramifying from the terminal crest toward the atrioventricular groove. In contrast, when the impulse reached the interatrial septum, slowing was often observed, suggesting that the septum acts as a barrier or sink for electrical current. We conclude that these inhomogeneities in atrial impulse propagation are consistent with existence of a specialized network of fast-conducting tissues. The purpose of these preferential pathways appears to be to assure synchronous atrial activation and contraction rather than rapid impulse conduction between the sinoatrial and atrioventricular nodes.

chick embryo; optical mapping; conduction system; internodal pathways; pectinate muscles

THE SPECIALIZED CONDUCTION tissues mediate coordinated propagation of electrical activity through the adult vertebrate heart. Although the ventricular component of the conduction system (His bundle, bundle branches, and Purkinje fibers) is relatively well characterized (reviewed in Ref. 14), controversy persists about the existence and even definition of specialized fast-conducting tissues within the atria (21). Inhomogeneities in conduction properties of atrial tissues are widely recognized and are believed to be largely due to structural characteristics (18). The morphological substrate of so-called internodal conduction tracts (20) is less well defined, since these bundles do not satisfy the criteria set for specialized ventricular conduction tissues (1).

Atrial conduction in adult human and animal hearts is well studied. Excitation starts in the sinoatrial node (or sinus venosus in the lower vertebrates) and propagates across the atrial roof in a generally radial manner, described as "waves produced when a stone is dropped into still water" (26). These "waves" are not perfectly concentric, since there are numerous "holes" in the atria where the veins enter (21), and spread of impulse appears to be faster along the main bundles of the pectinate muscles (2, 10, 26). In particular, the bundle of Bachman, located in the atrial roof, is implicated in connecting the left and right atrium electrically, thus assuring their almost simultaneous activation (1, 2). Elegant multielectrode mapping studies in the pig heart (3) have correlated preferential conduction pathways with areas of longitudinal myofiber orientation. In contrast, regions with complex orientation showed slowing or block of conduction. Thus myocardial geometry plays an important role in determining the atrial conduction patterns.

Conduction properties of the atrial myocardium change with development. In a study of directionality of impulse propagation during postnatal development in rabbits, cellular alignment, as well as localization of gap junctional proteins toward cell termini, was correlated with increased preferential conduction along the terminal crest (28). Information regarding conduction patterns in the prenatal atria is, however, sketchy. This is in large part because of technical challenges associated with studying these small, delicate, and spatially highly complex structures. The site of the first pacemaking activity has been localized to the left sinus horn in embryonic chick (23) and rat heart (17). Studies focused primarily on ventricular conduction depicted the activation of the atria proper from their upper right portion, proceeding toward the left side and the atrioventricular junction in both embryonic chick (32, 35) and rabbit (34) heart.

Our study sought to correlate structure with electrical activation by sequential mapping of developing chick atria during the stages preceding and covering the period of septation (HH16–HH36). Unlike the previous adult studies focused predominantly on the spread of activation from the sinoatrial node (6, 7, 11, 36), we devoted our attention to activation of atrial myocardium as a whole. Because of the known importance of myocardial arrangement for impulse propagation, we correlated activation maps with light, confocal, and electron microscopic images of the atrial architecture. We found that development of a preferential right-to-left conduction pathway

Address for reprint requests and other correspondence: D. Sedmera, Laboratory of Cardiovascular Morphogenesis, Institute of Animal Physiology and Genetics, Videnska 1083, 142 20 Prague 4-Krc, Czech Republic (e-mail: sedmera@iapg.cas.cz).

The costs of publication of this article were defrayed in part by the payment of page charges. The article must therefore be hereby marked "*advertisement*" in accordance with 18 U.S.C. Section 1734 solely to indicate this fact.

along the roof of the atria correlated with emergence of the pectinate muscles at stage 24. The spreading of excitation from the atrial roof toward the atrioventricular junction along the main bundles of pectinate muscles is consistent with a primary function of this system in assuring coordinated atrial contraction, similar to the function of the His-Purkinje system in the ventricles.

METHODS

Optical mapping. Techniques have been described in detail elsewhere (32). Setup for this study differed, since we used a 75-watt Xe lamp as a source of illumination and a 14-bit 80 × 80 pixel high-speed digital camera (RedShirt Imaging) as the imaging detector. Hearts from chick embryos between *incubation days 3* and *10* [HH16: N = 5, HH17 (8), HH21 (6), HH24 (6), HH25 (4), HH29 (8), HH31 (3), HH34 (10), and HH36 (5), staging according to Hamburger and Hamilton (HH; Ref. 16)] were isolated under a dissecting microscope and immersed in voltage-sensitive dye (0.002% Pyridinium, 4-(2-[6-(dibutylamino)-2-naphthalenyl]ethenyl)-1-(3-sulfopropyl)-hydroxide, inner salt (di-4-ANEPPS) in Tyrode-HEPES buffer, pH 7.4) for 5 min at room temperature. To reduce undesirable motion, we used cytochalasin D (4, 19) diluted from DMSO stock at a concentration of 20–40 μmol/l during the recordings. The hearts were then pinned in the desired orientation on the bottom of a silicone-lined custom-made copper dish with oxygenated Tyrode-HEPES solution positioned on a temperature-controlled stage (Biostage 600, 35°C) of an upright epifluorescence microscope (Leica DML-FS). With a green (546 ± 10 nm) excitation and red (590 nm LP) emission filter set, drop in fluorescence intensity corresponds to passing of action potential (Fig. 1). To accommodate hearts of different sizes, ×5, ×4, or ×2.5 dry objectives and ×0.24–0.38 photo tubes were used, resulting in individual pixel size between 13 and 42 μm. Images were recorded for 4 s in full-resolution mode (80 × 80 pixels) at 500–2,000 frames/s. Both anterior and posterior views of each heart were recorded. In addition, lateral and superior views with great arteries cut off were obtained in some hearts. Ectopic electrical pacing was performed as described previously (41) at different locations of both atria. Immediately after recordings were completed, high-resolution fluorescence images of the preparation were taken using the same objective with a 5-megapixel charge-coupled device camera (Canon PowerShot G5) for orientation.

Recordings were processed digitally using custom software (Cardioplex, running under an IDL 5.4 environment) bundled with the camera essentially as described previously (32, 42). The profiles of individual pixel intensity values over time were digitally filtered (Butterworth low-pass filter, cutoff at 100 Hz). No signal averaging was used; however, we determined empirically that the individual beats in the recorded sequence were virtually identical. Data sets acquired at 1,000 frames/s were used for analysis, since they represented the best compromise between signal quality and temporal resolution. The first derivative was computed for each channel, and its peak (the maximum upstroke velocity defined as dP/dt max) was used for construction of isochronal activation maps. Spatiotemporal filtering (3 × 3 Laplace) was used to smooth the contours. The activation maps were then manually superimposed on a high-resolution fluorescence image of the heart (Fig. 2). For display, the traces of individual channels were normalized, and movies of action potential propagation were constructed. For graphic visualization of the activation sequence, the image of the moving activation wavefront (the first derivative) was more informative, as demonstrated previously by others (46). The shape of isochrones was evaluated in ImageJ software using the area-to-perimeter ratio (roundness, or circularity).

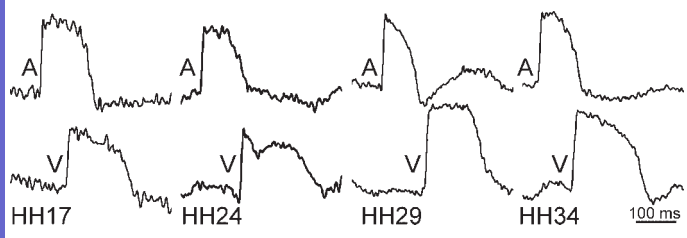

Fig. 1. Developmental differences in atrial (A)/ventricular (V) action potential morphology. Atrial action potentials are shorter than those in the ventricle and have a less prominent plateau phase. Note that the amplitude of optically recorded potentials is relative, reflecting mostly the amount of tissue under each pixel. HH, Hamburger and Hamilton stage.

Morphological examination. For evaluation of atrial myocardial architecture, we referred in part to specimens accumulated during previous studies. Scanning electron microscopy was used to assess the atrial endocardial aspect of specimens sectioned in the transverse, frontal, and sagittal plain in conjunction with study focused on ventricular myocardial architecture (38). Serial sections of embryos stained with MF20 monoclonal antibody (Developmental Studies Hybridoma Bank) detected by diaminobenzidine color reaction (39) were used to evaluate the development of pectinate muscles. The label-dilution technique, which highlights regions of nonproliferating cells associated with the developing conduction system (40, 44), was used to identify putative specialized conduction tissues within the atria. Existing serial sections, generated in previous studies (37, 45), were used for that purpose. Thick (200 μm) polyacrylamide sections of whole mount phalloidin-stained specimens (12) were examined by confocal microscopy to appreciate the three-dimensional architecture of the atrial muscle. Three-dimensional reconstruction was performed using Amira software on confocally sectioned whole mount specimens immunostained with MF20 and counterstained with propidium iodide (29). For each technique, a minimum of three embryos per stage was examined.

RESULTS

The optically recorded atrial action potentials showed generally lower amplitude than those from the ventricle (Fig. 1). The shape of the action potential was similar, except for the longer duration of the plateau phase in the ventricle. There were no remarkable differences in action potential shape with development or within the atria. Action potential duration tended to decrease with advancing development (R^2 = 0.68, Table 1), but exact quantification of this parameter is tricky, since we had to simultaneously increase the concentration of cytochalasin D, which does prolong action potential duration in the chick (32), to obtain sufficient motion control. Similarly, upstroke velocity quantification was not performed, since optically recorded action potentials are in relative values, which depend, among other things, on intensity of staining (higher at later stages) and numerical aperture of the objective used (lower at lower magnifications used at more advanced stages). Developmental changes in atrial activation patterns are depicted in Fig. 2. From the earliest stage studied, the first site of activation was located posteriorly on the right side of the midline slightly inferior to the roof. From there, the activation proceeded in both superior and inferior direction, resulting in the anterior surface being activated from the top toward the atrioventricular junction and from right to left. The time necessary for activation of the entire atrial surface decreased significantly between stages 17 and 24 (Table 1), indicating an increase in speed of conduction. Lateral views revealed that from stage 24 onward the first breakthrough on the left atrial surface occurred approximately one-third from the top, indicative of functionality of the emerging Bachman bundle (see

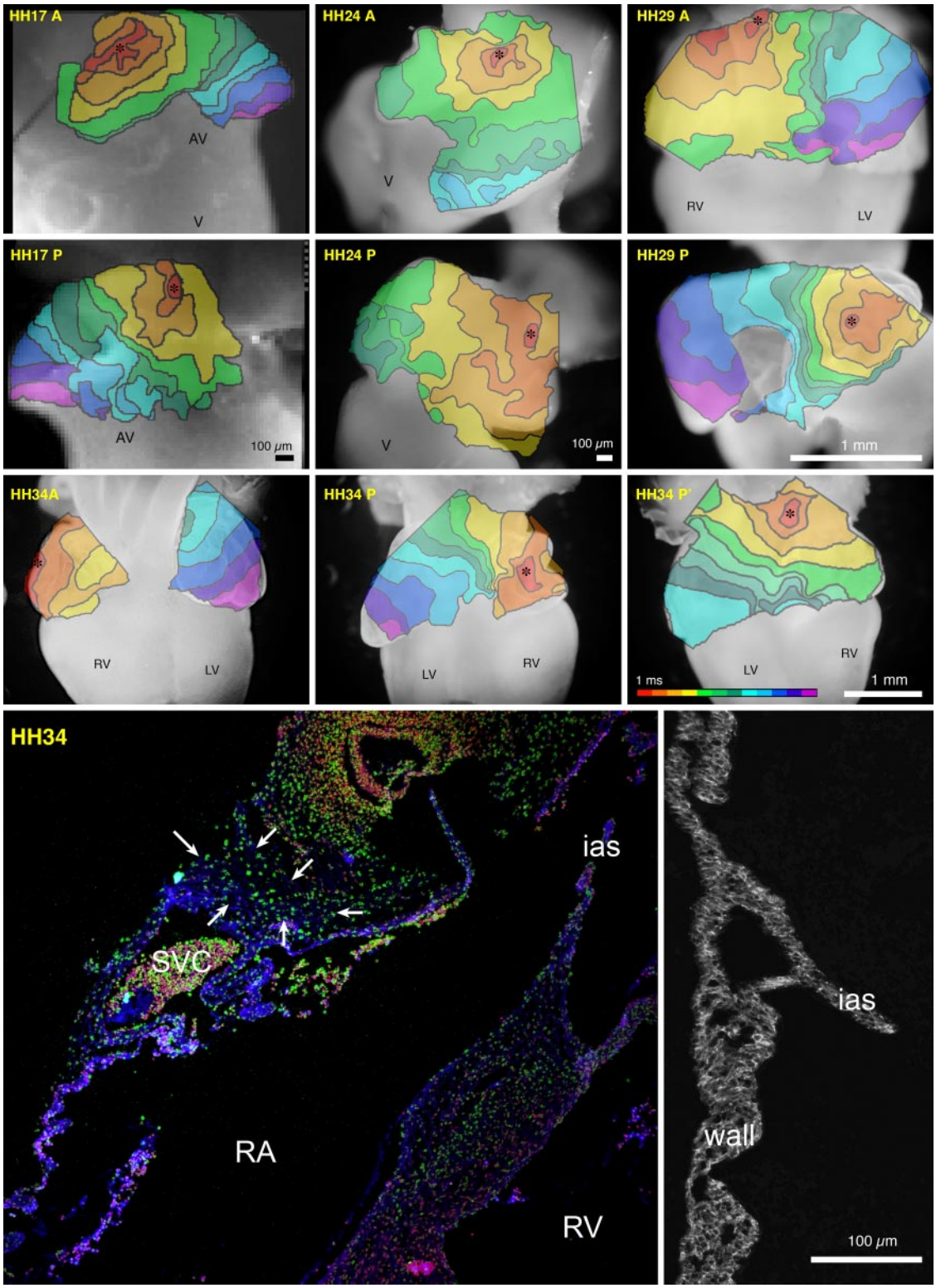

Fig. 2. Development of atrial activation sequence. Typical examples are shown from anterior (A) and posterior (P) aspects. In most cases, the outflow tract was cut off to provide an unobstructed view of the anterosuperior surface. *Earliest activated region. Isochrones (contours and color) are in 1-ms intervals. Scale bars 100 μm (HH17 and HH24) or 1 mm (HH29 and HH34); temporal color-coding is shown in the last panel. Two photomicrographs on *bottom* show the putative pacemaker region in the roof of the right atrium (RA) next to the entrance of the superior caval vein (SVC) and the detail of connection of the interatrial septum (ias) to the atrial wall. Green dots represent heavily labeled cells that did not further divide since the time of labeling (stage 16–20). Note that these cells form a cluster (white arrows), further distinguished by weak antimyosin labeling (blue). Red staining represents cell nuclei (propidium iodide). AV, atrioventricular canal, V, ventricle, LV, left ventricle, RV, right ventricle.

Table 1. *Quantitative analysis of atrial activation*

HH Stage	16/17	24/25	29	34	36
N	13	10	8	10	5
AP duration, ms	132±10	131±12	92±11	114±12	78±11
Activation time, ms	13±2	9±2†	12±2	11±2	13±2
Isochrone roundness (0-1)					
LA	0.36±0.10*	0.18±0.04	0.21±0.09	0.38±0.07	0.25±0.60
RA	0.67±0.03*	0.54±0.08	0.52±0.09	0.34±0.20	0.16±0.60

Values are means ± SE; *n,* no. of hearts. AP, action potential; LA, left atrium; RA, right atrium. The isochrones in both atria (examined from the posterior aspect) are significantly more regular at stage 16/17 before development of pectinate muscles. *$P < 0.05$ vs. subsequent stages. †$P < 0.05$ vs. stage 16/17 (unpaired 2-tailed *t*-test). HH stage, Hamburger and Hamilton stage.

supplemental movies at http://people.musc.edu/~sedmerad/animations/Supplemental atrial movies.html).[1] Frequency of this distinct pattern of activation increased from 5 to 10 hearts at stage 24/25, to 7 to 8 hearts at stage 29, and in all hearts examined at stages 24 and 36. The shape of isochrones became significantly more jagged at stage 24 when compared with stage 17 (Table 1). By stage 29, distinct slowing of the excitation wavefront was apparent around the interatrial septum. Total atrial activation time increased compared with stage 24, probably because of the doubling of atrial diameter. One-half of the hearts examined after stage 29 showed the first breakthrough on the posterior surface further inferiorly, overlying the crista terminalis and adjacent to the entrance of the inferior caval vein. This resulted in a more pronounced right-to-left activation pattern (Fig. 2, HH34P). However, in ~10% of hearts at all stages, the activation was proceeding from left to right, indicating a left-sided dominant pacemaker.

We were trying to better identify morphologically the region of the earliest activation (pacemaker site). Unfortunately, no connexins (gap junction proteins with differential expression between the working myocardium and conduction system; see Ref. 9) are detectable by immunohistochemistry in chick heart before stage 36/10 days of incubation (13). Using a label-dilution technique that highlights regions of cell quiescence such as early differentiating conduction tissues (44), we found a group of cells with weak anti-myosin staining and low proliferative activity in the roof and posterior wall of the right atrium adjacent to the entrance of the superior caval vein (Fig. 2). Although these characteristics, together with observed activation patterns, make this cluster of cells a strong candidate for the cardiac pacemaker, no distinct continuous tracts with these properties were detected within the atria (44).

Figure 3 shows an example of a scanning electron micrograph of the atrial endocardial surface during the later fetal stage (HH40, *day 14*). Pectinate muscles are prominent across most of the atria, with the thickest bundle running in the roof. Comparison with the anatomical atlas of the chick (25) showed that this arrangement is representative of the adult situation. Standard histology provided a useful complement to assess progression of atrial morphogenesis between HH17 and H34 (Fig. 4). At the earliest stage examined, the common atrium communicated widely with the sinus venosus, and the atrial wall of uniform thickness was formed by two to three cell layers of myocardium without epicardial coverage. By stage 24, the rudiments of pectinate muscles appeared in both atria, and the interatrial septum was now more distinct. The pectinate muscles increased rapidly in prominence, and, by stage 29, the adult pattern was essentially established, together with the venous connections to the atria (Fig. 5). By stage 34, some of the pectinate muscles exceeded the thickness of the atrial wall itself, whereas the interatrial septum was thin and fenestrated (Figs. 2, 4, and 5). Venous valves flanking the entrance of the inferior caval vein were other prominent ridge-like features in the atria (Figs. 4 and 5). Orientation of the myocytes in the atrium could be in general described as paralleling this of the pectinate muscles, i.e., circumferential from the roof toward the atrioventricular sulcus. However, the structure of the interatrial septum appeared much less directional, with numerous interatrial foramina (Fig. 5) giving it a sieve-like appearance.

Ectopic electrical pacing was performed in five hearts at stages 24 and 34 to determine if the observed patterns of

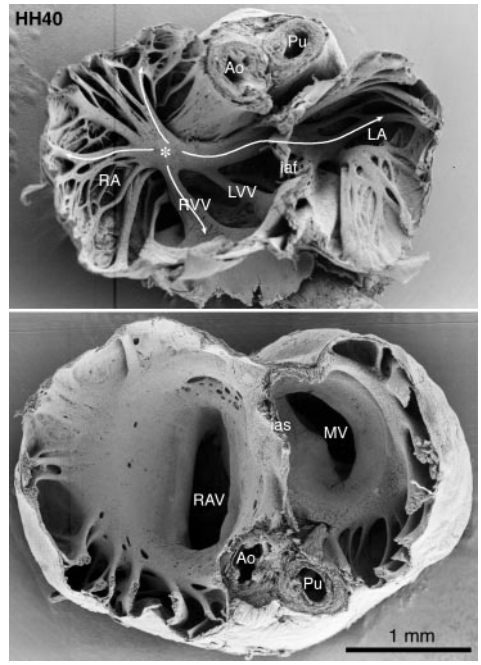

Fig. 3. Endocardial surface of late fetal chick atria. Bisection of the atria at *embryonic day 14* shows prominent interatrial bundle across the atrial roof (*top*). Main pectinate muscle bundles course from the area of the pacemaker (*) toward the atrioventricular junction. The arrangement is similar in the left atrium. Arrows indicate preferential spread of activation wavefront. Ao, aorta; iaf, interatrial foramina; LA, left atrium; LVV, left venous valves; MV, mitral valve; Pu, pulmonary artery; RA, right atrium; RAV, right atrioventricular valve; RVV, right venous valve.

[1] The online version of this article contains supplemental data.

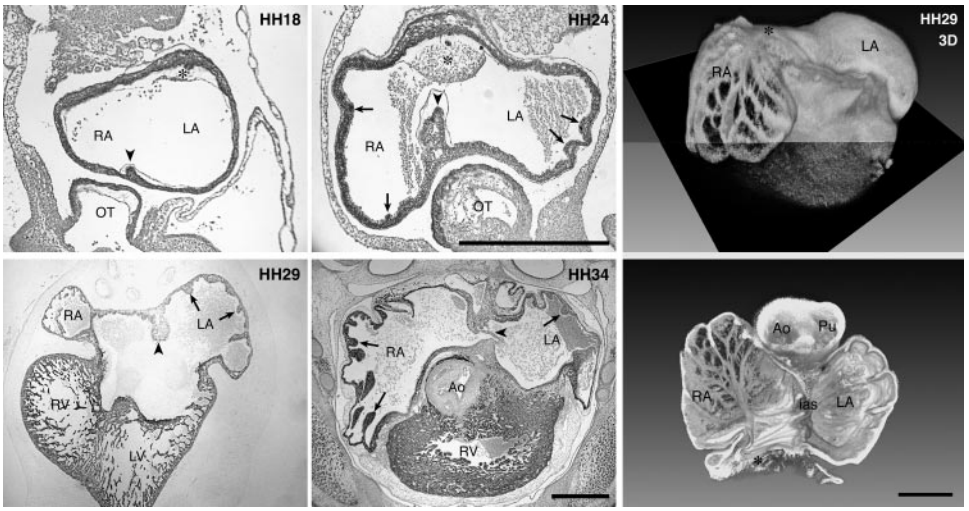

Fig. 4. Developmental changes in atrial myocardial architecture. Initially, the atrial wall is smooth with only a hint of the interatrial septum (HH18, arrowhead). Later on, folds corresponding to future pectinate muscles appear in both atria (HH24, arrows). These structures grow in prominence and complexity in both atrial chambers (HH29) until they get thicker than the atrial wall between them (HH34). Three-dimensional reconstruction shows that the definitive pattern of pectinate muscles is established by stage 29. Antimyosin heavy chain (MF20) staining; arrowheads, interatrial septum; arrows, pectinate muscles; OT, outflow tract. Scale bars 100 μm.

pectinate muscles correlated with anisotropy of impulse propagation. Total atrial activation time was slower by 20 and 30% compared with the spontaneous beat. In addition, although spontaneous activation showed faster propagation in the lateral (right to left) direction (1.25 and 1.42×, respectively) that parallels the crista terminalis and bundle of Bachman, paced beats induced in the middle of the anterior wall (both right or left) behaved in an opposite way, i.e., propagating faster along the pectinate muscles toward the atrioventricular sulcus than perpendicular to them (anisotropy 0.49 at stage 24 and 0.44 at stage 34, respectively, lateral vs. roof-to-sulcus direction).

DISCUSSION

Our study presents the first systematic description of atrial activation patterns during embryonic development in the chick in relation to changes in atrial myocardial architecture. Our data fully support the notion that geometry of muscle fibers is an important determinant of conduction properties of the atrial tissue (1). Since their earliest appearance, the nascent pectinate muscles show alignment with the direction of impulse propagation. This is in agreement with data obtained from a preparation of adult bullfrog atrium (10, 26) and sheep right atrium (2). The thickest parts of this system, the bundle of Bachman and the terminal crest, play an important role in interatrial transmission of the electrical impulse, similar to the situation described in humans (18). In contrast, the interatrial septum seems to act as a barrier to impulse propagation or an electrical sink (33), slowing the speed of propagation. The line of conduction block to the left of the sinoatrial node was previously described in the adult rabbit heart (5, 7, 11, 36), The

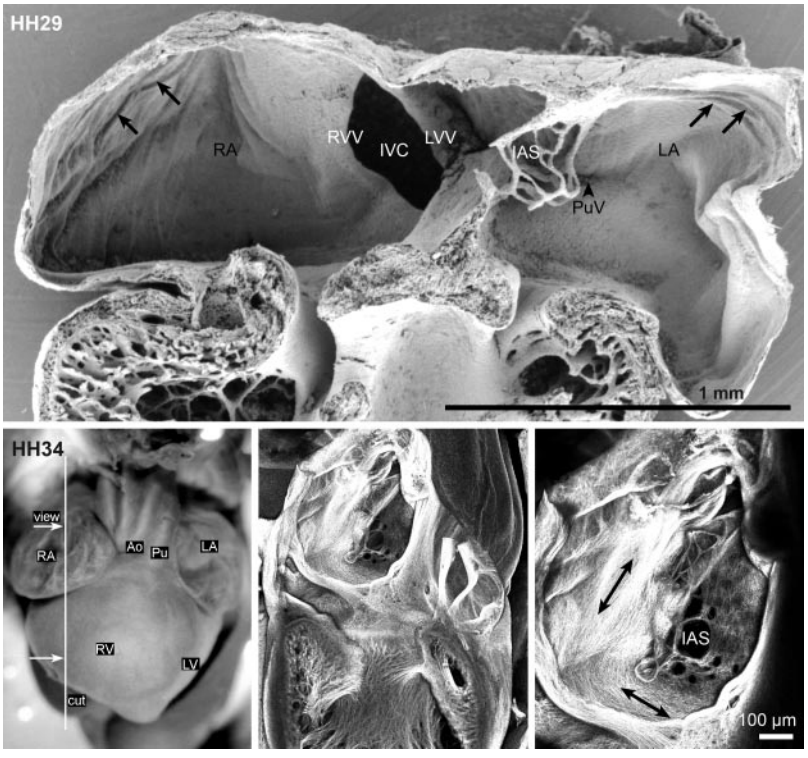

Fig. 5. Morphology of the interatrial septum. Scanning electron micrograph of dorsal half of frontally bisected stage 29 heart (*top*) shows multiple atrial fenestrations in the center of the septum. Note prominent ridges of the venous valves, flanking the slit-like entrance of the inferior caval vein (IVC) to the right atrium. The pectinate muscles (arrows) are visible in both atrial appendages. A single pulmonary vein (PuV) is seen in the posterior aspect of the left atrium. *Bottom*: sagittal dissection of stage 34 heart that exposes the interatrial septum from the right. Note that while the atrial myocytes are well aligned in this confocal projection of whole mount phalloidin staining (arrows), there is no predominant orientation in the septum (IAS) itself. Again, multiple interatrial foramina are seen.

substrate of this barrier, however, was not identified. Our study shows similar conduction patterns (Fig. 2); correlation with morphological examination suggests that the following several factors might participate: *1*) the interruption in the continuity of the right atrial wall caused by entrance of the inferior caval vein; *2*) prominent ridges of the right and left venous valves, flanking this opening; and *3*) adjacent interatrial septum, with a change in myocyte fiber orientation. Thus the easiest path connecting the right and left atrium is along the roof where there is a thick bundle of myocytes (Fig. 3).

It might be surprising to find considerable variability in the earliest site of activation on the posterior surface. However, the study of Betts and associates (3) showed that this is a rather normal feature even in the adult heart, since electrical mapping at the whole atrial level does not show the actual pacemaker site but rather the first activated region of working myocardium. The location of this site, however, is far from random, since it is always linked with the actual pacemaker site by a thick bundle of pectinate muscles. Given the rather high speed of impulse propagation throughout the atria, this variability seems to have little functional consequences for the pumping function, since the spread of excitation and ensuing contraction from either site are in agreement with blood flow toward the atrioventricular junction. Interestingly, ~10% of examined hearts, including those of embryonic rodents (40, 42), show left-to-right activation patterns. This could correspond to initially left-sided location of the earliest pacemaker described by Kamino and associates (17, 23) and, later on, the ring-like shape of the sinus venosus (30) that serves as a pacemaker. Normally, this activity is ultimately reorganized to the right-sided node, but occasional persistence of pacemaking tissues on the left side, including the orifice of the pulmonary vein(s), was attributed to atrial arrhythmias (31).

Although the histological markers we used to outline the pacemaking region (area of cell quiescence and low expression of sarcomeric proteins) might not be definitive proof of identity, a recent developmental study (47) showed that this region transiently expresses the hypoxia marker EF5, which marks other parts of the developing conduction system. Later on, a small branch of coronary artery, which is a landmark most anatomists would use to locate the sinoatrial node in the human heart, is consistently present. Thus, together with the activation maps, all these findings place the chick pacemaker at the roof of the right atrium, similar to the situation found in mammals (36).

Our data confirm the activation patterns recently reported in the chick by others (35) in both the right-to-left and top-to-bottom sequence as well as with the time period needed for atrial activation. Similar patterns have also been reported in embryonic rabbits (34) and rats (42), in both of which the activation of *embryonic day 14.5* atria shows distinct slowing across the interatrial septum and a predominantly right-sided origin. In addition to myofiber geometry, cell size appears to be a major factor for determination of the speed of impulse propagation (22, 43). However, this parameter changes little during prenatal development (24), and an increase in myocyte size resulting from hypertrophic growth occurs mostly after hatching (27). On the subcellular level, molecular heterogeneities play essential roles in determining conduction properties. During postnatal development of the terminal crest in rabbits, an increase in connexin 43 localization to the ends vs. the sides of the cardiomyocytes was correlated with increased directionality of impulse propagation (28). Connexin 40 is the second major gap junction protein strongly expressed in the atrium and is considered to be in part responsible for the conduction velocity that is higher than in the working ventricular myocardium, which expresses connexin 43 only (8). Electrophysiological studies in connexin 40-deficient mice (15) showed significantly decreased intra-atrial conduction velocity, which made them prone to burst pacing-induced arrhythmias. Unfortunately, we cannot correlate our data with connexin isoform expression, since the earliest connexin (42, cognate of mouse connexin 40) is detectable immunohistochemically in the chick only after *incubation day 10*. Apart from decreased conduction velocity, local obstacles creating blocks are another arrhythmogenic substrate; in that respect, pectinate muscles form barriers to impulse propagating perpendicular to their orientation (2), and breakdown of these natural barriers with the aging process could contribute to increased incidence of atrial arrhythmias with age. This suggests that substantial maturation of intra-atrial conduction pathways occurs postnatally (28). Our attempts at ectopic atrial pacing revealed significant slowing of propagation in the direction perpendicular to the main pectinate muscle bundles stretching from the atrial roof toward the atrioventricular sulcus. In addition, overall slowing of conduction velocity was noted, especially at increased pacing frequency. In conclusion, our study suggests that the developing myocardial architecture is the major determinant of atrial conduction and that the pectinate muscles play a role in coordinated spreading of electrical impulse through the atrial myocardium.

ACKNOWLEDGMENTS

We thank Carlin Rosengarten for help with analysis of the recordings.

GRANTS

This project was supported in part by National Institutes of Health Grants RR-16434, HL-50582, HL-52813, and HD-39446. D. Sedmera is currently supported by Grant VZ 206100–3 from the Ministry of Education of the Czech Republic, Institutional Research Plan IAPG AVOZ50450515 from the Academy of Sciences of the Czech Republic, and a Purkinje Fellowship from the Academy of Sciences of the Czech Republic.

REFERENCES

1. **Anderson RH and Ho SY.** The architecture of the sinus node, the atrioventricular conduction axis, and the internodal atrial myocardium. *J Cardiovasc Electrophysiol* 9: 1233–1248, 1998.
2. **Berenfeld O and Zaitsev AV.** The muscular network of the sheep right atrium and frequency-dependent breakdown of wave propagation. *Anat Rec A Discov Mol Cell Evol Biol* 280: 1053–1061, 2004.
3. **Betts TR, Ho SY, Sanchez-Quintana D, Roberts PR, Anderson RH, and Morgan JM.** Three-dimensional mapping of right atrial activation during sinus rhythm and its relationship to endocardial architecture. *J Cardiovasc Electrophysiol* 13: 1152–1159, 2002.
4. **Biermann M, Rubart M, Moreno A, Wu J, Josiah-Durant A, and Zipes DP.** Differential effects of cytochalasin D and 2,3 butanedione monoxime on isometric twitch force and transmembrane action potential in isolated ventricular muscle: implications for optical measurements of cardiac repolarization. *J Cardiovasc Electrophysiol* 9: 1348–1357, 1998.
5. **Bleeker WK, Mackaay AJ, Masson-Pevet M, Bouman LN, and Becker AE.** Functional and morphological organization of the rabbit sinus node. *Circ Res* 46: 11–22, 1980.
6. **Bleeker WK, Mackaay AJ, Masson-Pevet M, Op't Hof T, Jongsma HJ, and Bouman LN.** Asymmetry of the sino-atrial conduction in the rabbit heart. *J Mol Cell Cardiol* 14: 633–643, 1982.
7. **Boyett MR, Honjo H, Yamamoto M, Nikmaram MR, Niwa R, and Kodama I.** Downward gradient in action potential duration along con-

duction path in and around the sinoatrial node. *Am J Physiol Heart Circ Physiol* 276: H686–H698, 1999.
8. **Coppen SR, Kaba RA, Halliday D, Dupont E, Skepper JN, Elneil S, and Severs NJ.** Comparison of connexin expression patterns in the developing mouse heart and human foetal heart. *Mol Cell Biochem* 242: 121–127, 2003.
9. **Coppen SR, Severs NJ, and Gourdie RG.** Connexin45 (alpha 6) expression delineates an extended conduction system in the embryonic and mature rodent heart. *Dev Genet* 24: 82–90, 1999.
10. **Dillon S and Morad M.** A new laser scanning system for measuring action potential propagation in the heart. *Science* 214: 453–456, 1981.
11. **Efimov IR, Fahy GJ, Cheng Y, Van Wagoner DR, Tchou PJ, and Mazgalev TN.** High-resolution fluorescent imaging does not reveal a distinct atrioventricular nodal anterior input channel (fast pathway) in the rabbit heart during sinus rhythm. *J Cardiovasc Electrophysiol* 8: 295–306, 1997.
12. **Germroth PG, Gourdie RG, and Thompson RP.** Confocal microscopy of thick sections from acrylamide gel embedded embryos. *Microsc Res Tech* 30: 513–520, 1995.
13. **Gourdie RG, Green CR, Severs NJ, Anderson RH, and Thompson RP.** Evidence for a distinct gap-junctional phenotype in ventricular conduction tissues of the developing and mature avian heart. *Circ Res* 72: 278–289, 1993.
14. **Gourdie RG, Harris BS, Bond J, Justus C, Hewett KW, O'Brien TX, Thompson RP, and Sedmera D.** Development of the cardiac pacemaking and conduction system. *Birth Defects Res* 69C: 46–57, 2003.
15. **Hagendorff A, Schumacher B, Kirchhoff S, Luderitz B, and Willecke K.** Conduction disturbances and increased atrial vulnerability in Connexin40-deficient mice analyzed by transesophageal stimulation. *Circulation* 99: 1508–1515, 1999.
16. **Hamburger V and Hamilton HL.** A series of normal stages in the development of the chick embryo. *J Morphol* 88: 49–92, 1951.
17. **Hirota A, Kamino K, Komuro H, Sakai T, and Yada T.** Early events in development of electrical activity and contraction in embryonic rat heart assessed by optical recording. *J Physiol* 369: 209–227, 1985.
18. **Ho SY, Anderson RH, and Sanchez-Quintana D.** Atrial structure and fibres: morphologic bases of atrial conduction. *Cardiovasc Res* 54: 325–336, 2002.
19. **Jalife J, Morley GE, Tallini NY, and Vaidya D.** A fungal metabolite that eliminates motion artifacts. *J Cardiovasc Electrophysiol* 9: 1358–1362, 1998.
20. **James TN and Sherf L.** Specialized tissues and preferential conduction in the atria of the heart. *Am J Cardiol* 28: 414–427, 1971.
21. **Janse MJ and Anderson RH.** Specialized internodal atrial pathways: fact or fiction? *Eur J Cardiol* 2: 117–136, 1974.
22. **Jongsma HJ and Wilders R.** Gap junctions in cardiovascular disease. *Circ Res* 86: 1193–1197, 2000.
23. **Kamino K, Hirota A, and Fujii S.** Localization of pacemaking activity in early embryonic heart monitored using voltage-sensitive dye. *Nature* 290: 595–597, 1981.
24. **Knaapen MW, Vrolijk BC, and Wenink AC.** Nuclear and cellular size of myocytes in different segments of the developing rat heart. *Anat Rec* 244: 118–125, 1996.
25. **Komarek V, Malinovsky L, and Lemez L.** *Anatomia Avium Domesticarum et Embryologia Galli*. Bratislava, Slovakia: Priroda, 1982.
26. **Komuro H, Sakai T, Hirota A, and Kamino K.** Conduction pattern of excitation in the amphibian atrium assessed by multiple-site optical recording of action potentials. *Jpn J Physiol* 36: 123–137, 1986.
27. **Li F, McNelis MR, Lustig K, and Gerdes AM.** Hyperplasia and hypertrophy of chicken cardiac myocytes during posthatching development. *Am J Physiol Regul Integr Comp Physiol* 273: R518–R526, 1997.
28. **Litchenberg WH, Norman LW, Holwell AK, Martin KL, Hewett KW, and Gourdie RG.** The rate and anisotropy of impulse propagation in the postnatal terminal crest are correlated with remodeling of Cx43 gap junction pattern. *Cardiovasc Res* 45: 379–387, 2000.
29. **Miller CE, Thompson RP, Bigelow MR, Gittinger G, Trusk TC, and Sedmera D.** Confocal imaging of the embryonic heart: How deep? *Microscop Microanal* 11: 216–223, 2005.
30. **Moorman AF and Christoffels VM.** Cardiac chamber formation: development, genes, and evolution. *Physiol Rev* 83: 1223–1267, 2003.
31. **Pastelin G, Mendez R, and Moe GK.** Participation of atrial specialized conduction pathways in atrial flutter. *Circ Res* 42: 386–393, 1978.
32. **Reckova M, Rosengarten C, deAlmeida A, Stanley CP, Wessels A, Gourdie RG, Thompson RP, and Sedmera D.** Hemodynamics is a key epigenetic factor in development of the cardiac conduction system. *Circ Res* 93: 77–85, 2003.
33. **Rohr S, Kleber AG, and Kucera JP.** Optical recording of impulse propagation in designer cultures. Cardiac tissue architectures inducing ultra-slow conduction. *Trends Cardiovasc Med* 9: 173–179, 1999.
34. **Rothenberg F, Nikolski V, Watanabe M, and Efimov I.** Electrophysiology and anatomy of embryonic rabbit hearts before and after septation. *Am J Physiol Heart Circ Physiol* 288: H344–H351, 2005.
35. **Rothenberg F, Watanabe M, Eloff B, and Rosenbaum D.** Emerging patterns of cardiac conduction in the chick embryo: waveform analysis with photodiode array-based optical imaging. *Dev Dyn* 233: 456–465, 2005.
36. **Sano T and Yamagishi S.** Spread of excitation from the Sinus node. *Circ Res* 16: 423–430, 1965.
37. **Sedmera D, Hu N, Weiss KM, Keller BB, Denslow S, and Thompson RP.** Cellular changes in experimental left heart hypoplasia. *Anat Rec* 267: 137–145, 2002.
38. **Sedmera D, Pexieder T, Hu N, and Clark EB.** Developmental changes in the myocardial architecture of the chick. *Anat Rec* 248: 421–432, 1997.
39. **Sedmera D, Reckova M, Bigelow MR, DeAlmeida A, Stanley CP, Mikawa T, Gourdie RG, and Thompson RP.** Developmental transitions in electrical activation patterns in chick embryonic heart. *Anat Rec* 280A: 1001–1009, 2004.
40. **Sedmera D, Reckova M, DeAlmeida A, Coppen SR, Kubalak SW, Gourdie RG, and Thompson RP.** Spatiotemporal pattern of commitment to slowed proliferation in the embryonic mouse heart indicates progressive differentiation of the cardiac conduction system. *Anat Rec* 274A: 773–777, 2003.
41. **Sedmera D, Reckova M, DeAlmeida A, Sedmerova M, Biermann M, Volejnik J, Sarre A, Raddatz E, McCarthy RA, Gourdie RG, and Thompson RP.** Functional and morphological evidence for a ventricular conduction system in the zebrafish and *Xenopus* heart. *Am J Physiol Heart Circ Physiol* 284: H1152–H1160, 2003.
42. **Sedmera D, Reckova M, Rosengarten C, Torres MI, Gourdie RG, and Thompson RP.** Optical mapping of electrical activation in developing heart. *Microscop Microanal* 11: 209–215, 2005.
43. **Spach MS, Heidlage JF, Dolber PC, and Barr RC.** Electrophysiological effects of remodeling cardiac gap junctions and cell size: experimental and model studies of normal cardiac growth. *Circ Res* 86: 302–311, 2000.
44. **Thompson RP, Lindroth JR, and Wong YM.** Regional differences in DNA-synthetic activity in the presepatation myocardium of the chick. In: *Developmental Cardiology: Morphogenesis and Function*, edited by Clark EB and Takao A. Mount Kisco, NY: Futura, 1990, p. 219–234.
45. **Thompson RP, Reckova M, DeAlmeida A, Bigelow M, Stanley CP, Spruill JB, Trusk T, and Sedmera D.** The oldest, toughest cells in the heart. In: *Development of the Cardiac Conduction System*, edited by Chadwick DJ and Goode J. Chichester, UK: Wiley, 2003, p. 157–176.
46. **Vaidya D, Tamaddon HS, Lo CW, Taffet SM, Delmar M, Morley GE, and Jalife J.** Null mutation of connexin43 causes slow propagation of ventricular activation in the late stages of mouse embryonic development. *Circ Res* 88: 1196–1202, 2001.
47. **Wikenheiser J, Doughman YQ, Fisher SA, and Watanabe M.** Differential levels of tissue hypoxia in the developing chicken heart. *Dev Dyn* 235: 115–123, 2006.